

# Accuracy and precisions of water quality parameters retrieved from Particle Swarm Optimisation in a sub-tropical lake

Glenn Campbell<sup>\*ab</sup> and Stuart R. Phinn<sup>a</sup>

<sup>a</sup> University of Queensland, Centre for Remote Sensing and Spatial Information Science, School of Geography, Planning and Environmental Management, St Lucia QLD 4072

<sup>b</sup> University of Southern Queensland, Australian Centre for Sustainable Catchments & Faculty of Engineering and Surveying, Toowoomba QLD 4350

## ABSTRACT

Optical remote sensing has been used to map and monitor water quality parameters such as the concentrations of hydrosols (chlorophyll and other pigments, total suspended material, and coloured dissolved organic matter). In the inversion / optimisation approach a forward model is used to simulate the water reflectance spectra from a set of parameters and the set that gives the closest match is selected as the solution. The accuracy of the hydrosol retrieval is dependent on an efficient search of the solution space and the reliability of the similarity measure. In this paper the Particle Swarm Optimisation (PSO) was used to search the solution space and seven similarity measures were trialled. The accuracy and precision of this method depends on the inherent noise in the spectral bands of the sensor being employed, as well as the radiometric corrections applied to images to calculate the subsurface reflectance. Using the Hydrolight® radiative transfer model and typical hydrosol concentrations from Lake Wivenhoe, Australia, MERIS reflectance spectra were simulated. The accuracy and precision of hydrosol concentrations derived from each similarity measure were evaluated after errors associated with the air-water interface correction, atmospheric correction and the IOP measurement were modelled and applied to the simulated reflectance spectra. The use of band specific empirically estimated values for the anisotropy value in the forward model improved the accuracy of hydrosol retrieval. The results of this study will be used to improve an algorithm for the remote sensing of water quality for freshwater impoundments.

**Keywords:** Particle Swarm Optimisation, water quality, error assessment, MERIS, inland waters

## 1 INTRODUCTION

Optical remote sensing has been used to retrieve water quality parameters such as the concentrations of hydrosols (chlorophyll and other pigments, total suspended material, and coloured dissolved organic matter) to model dynamic environmental processes.

The subsurface reflectance spectrum ( $R(\lambda, \theta)$ ) is a result of the cumulative interactions of light with the water itself and the hydrosols. To retrieve the hydrosol concentrations it is necessary to invert the reflectance spectrum. The hydrosol concentrations and the reflectance spectrum are linked by the inherent optical properties (IOPs) of the water. These three properties have magnitudes that are independent of the geometric structure of the light field. The absorption coefficient ( $a$ ) describes the probability of a photon being absorbed, the scattering coefficient ( $b$ ) describes the probability of a photon being scattered and the volume scattering function (VSF) ( $\beta(\theta)$ ) describes the probability of a scattered photon being scattered in a particular direction. The last two properties are usually combined into the total backscattering probability ( $b_b$ ) which describes the probability of a photon being scattered in a direction greater than  $90^\circ$  to its initial direction of travel. Any successful semi-analytic inversion approach needs to relate the reflectance to the IOPs and then the IOPs to the hydrosol concentrations.

Each natural water body, via the water IOPs, has distinctive relationships between hydrosol concentrations and the remotely sensed reflectance. In the inversion / optimisation approach a forward model is used to simulate the spectra from a number of parameters and the set of parameters that minimises a selected cost function are selected as the solution. This approach can be divided into subgroups. The inversion approach directly inverts the model to recover the

---

\* Glenn.Campbell@usq.edu.au; Tel: +61 7 4631 2909 Fax: +61 7 4631 2526

hydrosol values and the optimisation approach uses a forward model to calculate a reflectance spectrum from hydrosol values and then uses a similarity measure to match it to the measured reflectance spectrum.

This paper uses the average retrieval error and its 95% confidence interval as a measure of the efficacy of spectral similarity measures. It investigates how these measures are affected by uncertainty in the measured reflectance spectrum and the model parameters. It also considers the utility of the sensor to retrieve hydrosol concentrations for Wivenhoe Dam, a large freshwater storage in South East Queensland.

### 1.1 Study Site and Field Measurements

Lake Wivenhoe is located in the upper Brisbane River in South East Queensland, Australia. Risk assessments based on waterbody morphology, hydrographic relations between the catchment area and the waterbody and the antropogenic nutrient load [1] characterise the overall water quality rating as moderate and the cyanobacterial rating as poor [2].

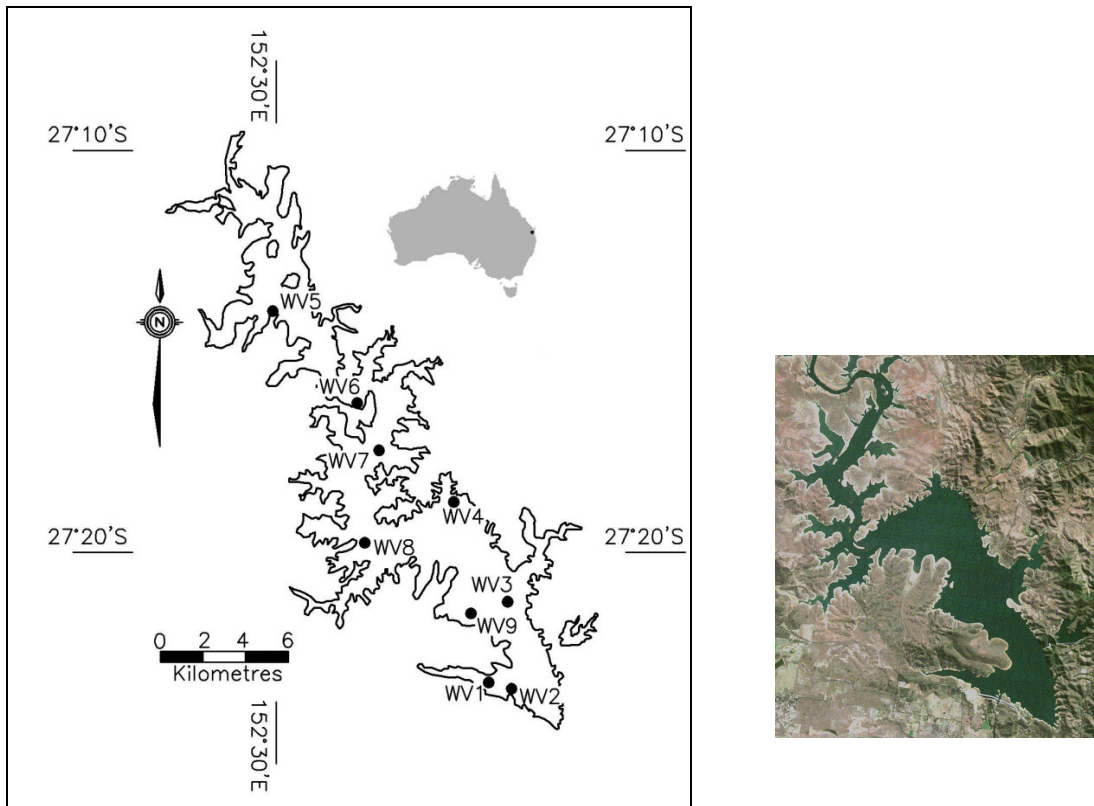


Fig. 1 Location of the SIOP sample sites for the July 2007 fieldwork activities on Wivenhoe Dam, Australia. The left hand image shows the calculated full supply level and the right hand side shows a Landsat true colour image of the reduced water extent at the time of the fieldwork activities.

During July 2007 the IOPs of the storage were measured at nine stations (Fig. 1) between the dam wall and the Esk offtake tower (WV5). Water samples were taken from the near surface water and kept cool for later laboratory measurement of total suspended material (TSM), chlorophyll *a* (CHL) concentration and CDOM concentration. The spectral absorption of the hydrosols was measured with a UV/VIS dual beam spectrophotometer with integrating sphere[3]. At each station the water was pumped for a minimum of ten minutes from approximately 0.5m below the surface, settled to remove air bubbles and then gravity fed successively through a conductivity-temperature sensor and a *WET Labs* absorption and attenuation meter (ac-9) [4] and finally emptied into a black plastic container. In the container the scattering properties were measured using a HydroScat-6 [5]. A separate measurement of the backscattering of phytoplankton cells was not feasible; the assumption was made that  $1 \mu\text{g l}^{-1}$  of CHL was approximately equal to  $0.07 \text{mg l}^{-1}$  TSM [6].

## 1.2 Reflectance Spectra Simulation

The subsurface reflectance was modelled with *Hydrolight 4.2*®, a numerical model which solves the radiative transfer equation to produce radiance distributions and derived quantities for natural waters [7].

Based on monitoring data over the last 5 years supplied by SEQWater *Hydrolight*® simulations were run at the hydrosol concentration values and the sun positions shown in Table 1. As SEQWater does not regularly measure CDOM values the range was estimated based on field measurements. Freshwater absorption [8, 9] and backscattering [9] values were taken from literature.

Table 1: Hydrosol concentrations and sun positions used in simulation of the reflectance spectra

Hydrosol	Concentration
Chlorophyll <i>a</i> ( $\mu\text{g l}^{-1}$ )	0,2,4,6,8,10,12,14,16,18,20
TSM ( $\text{mg l}^{-1}$ )	0,2,4,6,8,10,12,14,16,18,20
CDOM ( $a_{\text{CDOM @440 nm}} [\text{m}^{-1}]$ )	0,0.1,0.2,0.3,0.4,0.5,0.6,0.7,0.8
Sun zenith Angle ( $^{\circ}$ )	0,9.5,19.1,29.0,36.9,43.5,49.5,54.9,61.1

The simulations used average IOP values from the 2007 site visit at 1nm steps between 401-799nm using a clear sky with the default *Hydrolight*® atmosphere, an infinite depth and a windspeed of 1m/s. To model the effect of the sun position nine simulation sets were run for clear skies with the sun zenith angle varying from  $0^{\circ}$  to  $61.1^{\circ}$ . The angles were selected so that their secants were evenly distributed. The simulated spectra were then convolved with the first twelve MERIS bands (412.5nm, 442.5nm, 490nm, 510nm, 560nm, 620nm, 665nm, 681.25nm, 708.75nm, 753.75nm, 760.625nm and 778.75nm).

## 2 OPTIMISATION

### 2.1 Bio-Optical Model

The most common semi-analytical model for in-water reflectance was developed by Gordon, Brown and Jacobs [10] using the optical depth  $\tau$  as the independent variable.

$$R(\tau, -) = \sum_{n=0}^N r_n(\tau) X^n, \quad X = \frac{\omega_0 B}{(1 - \omega_0 F)}, \quad \tau = \int_0^z c(z) dz \quad (1)$$

$B$  and  $F$  are the backscattering and forward scattering probabilities and  $\omega_0$  is the ratio between the total scattering coefficient  $b$  and the total attenuation co-efficient  $c$ . The constants in polynomial equation  $r_n(\tau)$  are dependent on the illumination conditions. The dependence on wavelength has been omitted for clarity. As  $B=1-F$  the equation can be represented in the more common form [11].

$$R(\lambda, 0^-) = \sum_{n=0}^{n=3} f_n(\lambda) [\omega_b(\lambda)]^n, \quad \omega_b(\lambda) = \frac{b_b(\lambda)}{a(\lambda) + b_b(\lambda)} \quad (2)$$

The proportionality factor  $f$  is often referred to as the anisotropy factor as it represents a correction for the direction distribution of light in the upwelling and downwelling fields. From the result of the *Hydrolight*® simulations values for  $f_n$  were calculated for a quadratic and cubic equation for  $R(0^-)$  in terms of  $\omega_b$  for each sun position.

A four part absorption model was used.

$$a(\lambda) = a_w(\lambda) + a_{\text{CDOM}}(\lambda) + a_{\text{TSM}}(\lambda) + a_{\phi}(\lambda) \quad (3)$$

The values for  $a_w(\lambda)$  were obtained from Pope and Fry [8]. The absorption due to CDOM, TSM and Chlorophyll  $a_{\phi}$  is proportional to the concentration of the constituent. This is normally represented by the use of a specific absorption coefficient ( $a^*$ )

$$a_i(\lambda) = C_i a_i^*(\lambda). \quad (4)$$

The specific spectra were sourced from averaging the spectra obtained from the field measurements described earlier in the text.

A three part backscattering model was used.

$$b_b(\lambda) = b_{bw}(\lambda) + b_{bTSM}(\lambda) + b_{b\phi}(\lambda). \quad (5)$$

The scattering coefficient for pure water was obtained from Morel [12] and a ratio of  $b_w:b_{bw}$  of 0.5 was used. The backscattering of TSM and phytoplankton were obtained from averaging the measured field samples and calculating the specific coefficients as before. Plots of the average SIOPs for Wivenhoe Dam are shown in Fig. 2.

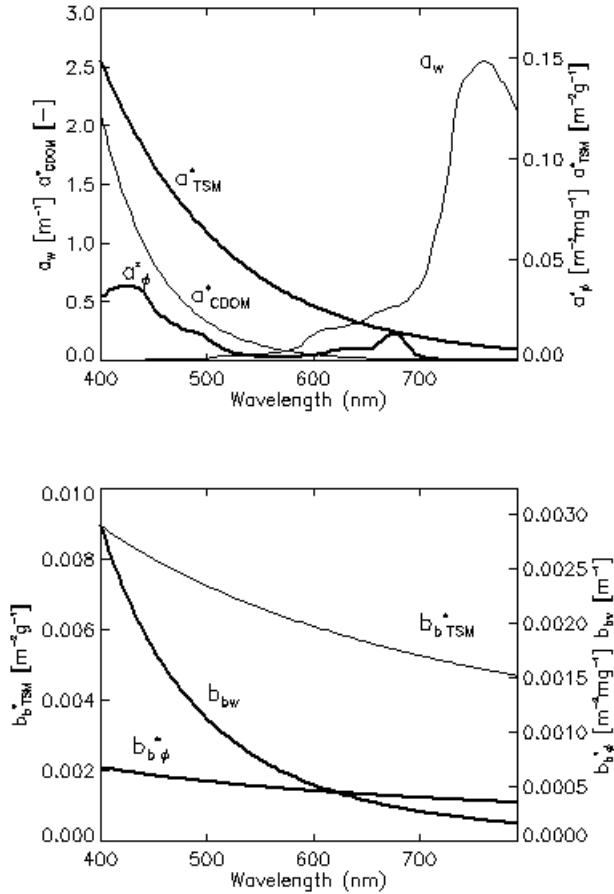


Fig. 2: Average SIOPs for Wivenhoe Dam: The upper graph shows the spectral absorption of water ( $w$ ) and the specific absorption spectra of chlorophyll  $a$  ( $\phi$ ), total suspended material ( $TSM$ ) and coloured dissolved organic matter ( $CDOM$ ). The lower shows the spectral backscattering of water ( $w$ ) and the specific backscattering spectra of chlorophyll  $a$  ( $\phi$ ) and total suspended material ( $TSM$ ).

## 2.2 Anisotropy factor

Aas [13] showed that the anisotropic factor was related to shape factor for scattering in the upward ( $r_u$ ) and downward ( $r_d$ ) direction. These are often assumed to be constant but  $r_d$  of 1.3-10 and  $r_u$  of 1.8-20 have been modelled for the development of a *Platymonas* algal bloom in Case I waters [14]. The shape factors rose slowly as the chlorophyll  $a$  plus phaeopigments concentration increased until it reached 0.1 mgm<sup>-3</sup> then the shape factors increased exponentially. The use of a constant anisotropy factor may have a significant effect on the model accuracy.

The shape of the light field will be dependent on the scattering and absorption IOPs of the water and the hydrosols in question as well as the illumination properties. As the IOPs are not spectrally invariant, it is logical to presume that the

shape of the light field for each wavelength will be different. The parameters of the polynomial fit for  $R(\theta)$  in terms of  $\omega_b$  will reflect the shape of the light field and hence the relationship between  $R(\theta)$  and  $\omega_b$  is not spectrally invariant either. The hypothesis is that calculating band specific polynomial fits will increase the accuracy and precision of the final retrieval.

### 2.3 Particle Swarm Optimisation (PSO)

The PSO is the stochastic search technique which includes a random element in the search approach that was first applied to ocean colour by Slade et al. [15]. The algorithm represents the solution as an  $n$ -dimensional vector in an  $n$ -dimensional solution space. It then mimics the action of a swarm by generating a number of potential solutions or ‘particles’ and after each iteration having them react to the closest match in its local area as well as the best match from all the particles. The best match can be defined by any appropriate cost function or similarity measure.

Let  $\mathbf{x}_j$  be a particle and the position of  $\mathbf{x}_j$  after the next iteration as  $\mathbf{x}_j + \Delta \mathbf{x}_j$  where  $\Delta \mathbf{x}_j$  is referred to as the trajectory. The trajectory is related to the value of two vectors, the vector connecting  $\mathbf{x}_j$  to the best match that it has previously made ( $\mathbf{x}_{j,best}$ ) by that particle and the vector connecting  $\mathbf{x}_j$  to the best match that any of the particles have made ( $\mathbf{x}_{G,best}$ ). The random element is introduced by generating random number multiples of the components of  $\mathbf{x}_{j,best}$  and  $\mathbf{x}_{G,best}$ . The bias towards each component vector is controlled by two weight constants  $c_1$  and  $c_2$ . To aid in the convergence the sum of the vectors is multiplied by a constriction factor  $\chi$ .

Formally,

$$\mathbf{x}_j(t+1) = \mathbf{x}_j(t) + \Delta \mathbf{x}_j(t+1) \tag{6}$$

$$\Delta \mathbf{x}_j(t+1) = \chi (\Delta \mathbf{x}_j(t+1) + \Phi_1(\mathbf{x}_{j,best} - \mathbf{x}_j(t)) + \Phi_2(\mathbf{x}_{G,best} - \mathbf{x}_j(t))) \tag{7}$$

In this case the search space is three dimensional so

$$\Phi_m = c_m \begin{bmatrix} r_{m,1} & 0 & 0 \\ 0 & r_{m,2} & 0 \\ 0 & 0 & r_{m,3} \end{bmatrix} \text{ where } r_{m,i} \text{ are random scalars uniformly distributed between 0 and 1.}$$

$$\chi = \frac{2}{|2 - \phi - \sqrt{\phi^2 - 4\phi}|} \quad \phi = c_1 + c_2, \quad \phi > 4 \tag{8}$$

The  $\phi > 4$  restriction is required to prevent the values of the trajectories from becoming cyclical and hence not randomly searching the solution space [16]. The parameters  $c_1$  and  $c_2$  were set at 2.05 [15] and a swarm of 27 particles was used. Fig. 3 shows a graphical representation of the particle trajectory update.

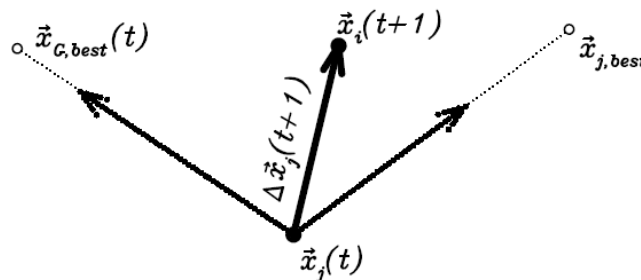


Fig. 3 Graphical representation of the calculation of the particle trajectory.

## 2.4 Similarity Measures

The PSO determines the direction of the search based on the values of the best spectrum match. These values can be provided by any number of similarity measures. Four similarity measures and their combinations were tested to see which returned the most accurate and precise results.

### 2.4.1 Spectra Angle Mapper

The Spectra Angle Mapper (SAM) measure treats the two spectra as  $n$ -dimensional column vectors and uses their dot product normalised for the magnitude of the vectors as a measure of their similarity.

Formally let  $\mathbf{x}$  and  $\mathbf{x}'$  be two spectra with  $n$  bands then

$$SAM(\mathbf{x}, \mathbf{x}') = \cos^{-1} \left( \frac{\sum_{i=1}^n x_i x'_i}{\sqrt{\sum_{i=1}^n x_i^2} \cdot \sqrt{\sum_{i=1}^n x_i'^2}} \right) \quad (9)$$

### 2.4.2 Spectral Information Divergence

The Spectral Information Divergence (SID) is a stochastic rather than deterministic measure of similarity [17]. It reduces the vectors to probability vectors before comparing them. This is achieved by normalising the vector by dividing by the sum of its components. For a given band this probability can be converted into its self-information. In broad terms this describes the unlikeliness of the predicted outcome. The discrepancy in a particular band is the difference between the self information of the comparable bands in the two spectra. The discrepancy of the spectra is the sum of the band discrepancy weighted by that band's probability. For this reason the discrepancy is not commutative so the SID is calculated as the sum of the discrepancies of the two combinations.

Formally, let  $\mathbf{x}$  and  $\mathbf{x}'$  be two spectra with  $n$  bands with probability vectors  $\mathbf{p}$  and  $\mathbf{q}$  respectively. The probability for a given band is:

$$p_i = \frac{x_i}{\sum_{i=1}^n x_i} \text{ and the self-information for each band is } I_i(\mathbf{x}) = -\log(p_i).$$

The discrepancy of a band is  $D_i(\mathbf{x} \parallel \mathbf{x}') = I_i(\mathbf{x}) - I_i(\mathbf{x}') = \log\left(\frac{p_i}{q_i}\right)$  and the discrepancy of the spectra is

$$D(\mathbf{x} \parallel \mathbf{x}') = \sum_{i=1}^n p_i \log\left(\frac{p_i}{q_i}\right). \quad (10)$$

Lastly,

$$SID(\mathbf{x}, \mathbf{x}') = D(\mathbf{x} \parallel \mathbf{x}') + D(\mathbf{x}' \parallel \mathbf{x}) \quad (11)$$

### 2.4.3 Spectral Correlation Mapper

The Spectral Correlation Mapper (SCM) is a modification of the SAM that takes into account the sign of the correlation not just the magnitude [18].

$$SCM(\mathbf{x}, \mathbf{x}') = \cos^{-1} \left( \frac{\sum_{i=1}^n (x_i - \bar{x})(x'_i - \bar{x}')}{\sqrt{\sum_{i=1}^n (x_i - \bar{x})^2} \cdot \sqrt{\sum_{i=1}^n (x'_i - \bar{x}')^2}} \right) \quad (12)$$

### 2.4.4 Minimum Distance

The three previous measures mathematically eliminate the magnitude of the reflectance spectra from the calculation and focus on its shape. However, as the TSM concentration increases in water, the increased scattering leads the reflectance spectra to increase in magnitude rather than change in shape. The minimum distance measure only considers the magnitude of the two spectra by calculating the Euclidean distance between their vectors in band space.

$$MIN(\mathbf{x}, \mathbf{x}') = \sqrt{\sum_{i=1}^n (x_i^2 - x_i'^2)} \quad (13)$$

### 2.4.5 Combined Measures

The combinations were simple multiplications except for

$$SIDSAM = SID \cdot \tan(SAM) \quad [17]. \quad (14)$$

### 2.5 Simulation of Noise

The bio-optical models described above relate the subsurface reflectance to the absorption and backscattering of the water and hydrosols. As a remote sensor measures the top of atmosphere radiance, the effect of the atmosphere and the air-water interface must be eliminated before the subsurface reflectance spectra can be used. In addition the inversions rely on having accurate specific absorption and backscattering spectra. Any measurement errors, approximations or assumptions made in this process will introduce error into the retrieved hydrosol concentrations. The ability of a similarity measure to alleviate the effect of these errors will be a useful measure of its efficacy.

To simulate the effect of three broad types of error the following distortions were made to the simulated spectra or the SIOPs:

### 2.6 Environmental noise errors

Some errors act separately in each band meaning the reflectance spectra is distorted in shape as well as scale. Some of the sources of this variation are:

- A single value of the ratio of upwelling irradiance to upwelling radiance ( $Q$ ) is used in the air-water interface correction of De Haan & Kokke [19] but the Hydrolight simulations show this value varies by approximately 4.6% (range 4.52- 4.96) .
- The average error between the fitted curve and the raw data for the anisotropy factor  $f$  was 1%.
- The environmental noise-equivalent radiance difference ( $NEAR(O)_E$ ) is the standard deviation of the subsurface reflectance in each band over a homogeneous area of optically deep water [20]. Using a MERIS full resolution image acquired on the 2 July 2007 corrected using c-WOMBAT-c [20] the  $NEAR(O)_E$  was estimated to be a constant 0.1% in all bands.

For eight noise levels between 0-7% these errors were imitated by adding in a simulated spectrum a normally-distributed, pseudo-random number with a mean of zero and a standard deviation of one that was scaled to the particular noise level of each band. An offset representing the  $NEAR(O)_E$  was then applied. As each band had a different scale factor applied to it the effect was to distort the shape as well as the scale of the spectra. The inversion was run on the 9801 simulated spectra with 50 applications of the noise. The inversion algorithm was applied and the mean of the 50 mean errors was calculated for each hydrosol value at each noise level.

### 2.7 Atmospheric correction errors

The errors associated with the atmospheric correction involve a scale error and a shape error as before but in this case the amount of the error in each band will be correlated. In broad terms the scale error will occur when an incorrect estimate has been made of the visibility and the shape error will occur from making a poor estimation of the aerosol types or their mixing ratio. The spectral dependence of the path radiance conforms to a power law so the spectra were modified by single scale variable (0-20%, normally distributed) as well as a value for the slope (0-10%) The inversion was run as described in the previous section.

### 2.8 SIOP measurement errors

The PSO method requires that the spectra for  $a^*$  and  $b^*_b$  be calculated from field measurement of the total absorption and backscattering for each constituent and the hydrosol concentration. Measurement errors in the hydrosol concentration will result in a consistent scale error across all bands as the hydrosol concentration is used as a divisor for each band when the SIOP is calculated. In addition, the measurement of absorption and backscattering for each constituent will have a shape error associated with it due to random errors in their measurement. For the phytoplankton absorption the shape change was modelled in the same way as the signal shape error. The other hydrosols' absorption and the backscattering calculations involve fitting a function with slope and scale parameters to the raw observation so their errors were modelled using a variation of spectral slope in the same way as the atmospheric correction error. After considering the variation in SIOPs measured during the July 2007 site visit, the phytoplankton SIOP scale error bounds

were set to 0% and 20% and the noise applied to the slope was set at half the value for the scale. The absorption and scattering of pure water was not varied. The inversion was run as described in the previous section.

### 3 RESULTS

The PSO is a stochastic search technique which includes a random element in the search approach. This means the path of each particle is different each time the optimisation is run. As an example, Fig. 4 below shows the four search path for the same starting particle matching the same input spectra using the SID matching condition. The starting point is Chlorophyll *a* 5  $\mu\text{g l}^{-1}$ , TSM 5  $\text{mg l}^{-1}$ , and CDOM 0.25  $\text{m}^{-1}$ . The final solution is the same, Chlorophyll *a* 3.66  $\mu\text{g l}^{-1}$ , TSM 16.08  $\text{mg l}^{-1}$ , and CDOM 0.64  $\text{m}^{-1}$  and the true value is Chlorophyll *a* 4  $\mu\text{g l}^{-1}$ , TSM 16  $\text{mg l}^{-1}$ , and CDOM 0.6  $\text{m}^{-1}$

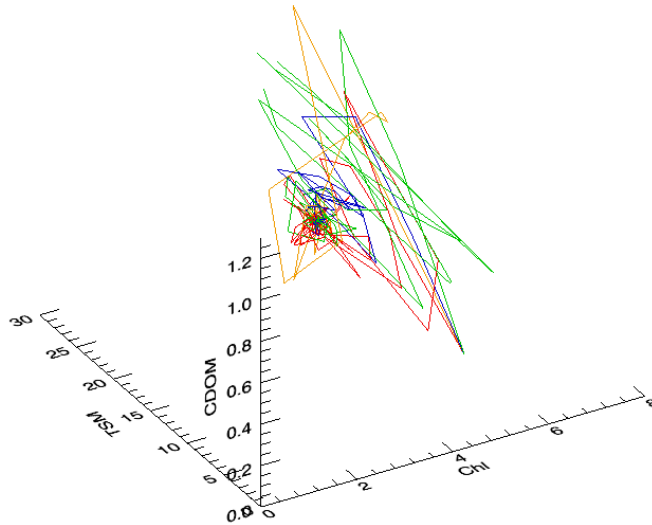


Fig. 4: Trajectory of a single particle during four inversions of the same spectrum.

#### 3.1 Baseline Accuracy

The baseline values for the PSO are reported in Table 2 and Table 3 for the quadratic and cubic formulations of the forward model. It is clear that the band specific cubic function is superior for all of the matching criteria. It will be used in the estimation of effects of the other noise sources.

Table 2: Means of the means of the absolute values of error for inversions at nine different sun angles using a single parameter function for all bands. \* denotes the difference is not significant at 95%. The best result for each hydrosol is shown bold.

	Cubic Function						Quadratic Function					
	Chl		TSM		CDOM		Chl		TSM		CDOM	
	Av	SD	Av	SD	Av	SD	Av	SD	Av	SD	Av	SD
SID	0.29	0.41	0.16	0.18	0.02	0.05	1.35	1.75	0.31	0.36	0.06	0.09
SAM	<b>0.19</b>	<b>0.46</b>	<b>0.11</b>	<b>0.20</b>	0.03*	0.06	0.80	1.23	0.22	0.35	0.05	0.08
MIN_DIST	0.28	0.96	0.19	0.16	0.03	0.03	0.67	1.26	0.19	0.16	0.03	0.04
SIDSAM	0.25	0.47	0.14	0.20	0.02	0.06	1.13	1.49	0.25	0.35	0.05	0.09
SIDMIN	0.20	0.30	0.18	0.15	<b>0.02</b>	<b>0.02</b>	0.87	1.24	0.24	0.30	0.04	0.08
SAMMIN	0.22	0.72	0.18	0.14	0.03*	0.06	0.63	1.00	0.18	0.15	0.03	0.04
SCM	0.32	0.44	0.22	0.24	0.05	0.06	0.34	0.60	0.60	0.44	0.10	0.08

Table 3: Means of the means of the absolute values of the error for inversions at nine different sun angles using separate parameter functions for each band. \* denotes the difference is not significant at 95%. The best result for each hydrosol is shown bold.

	Band Specific Cubic Function						Band Specific Quadratic Function					
	Chl		TSM		CDOM		Chl		TSM		CDOM	
	Av	SD	Av	SD	Av	SD	Av	SD	Av	SD	Av	SD
SID	0.16	0.63	0.09	0.21	0.02*	0.07	0.23	0.35	0.12	0.20	0.02	0.06
SAM	0.23	1.12	0.11	0.28	0.02	0.08	0.21	0.36	0.13	0.22	0.02	0.06
MIN_DIST	0.24	1.04	0.17	0.16	0.03	0.03	0.40	1.05	0.18	0.16	0.03	0.04
SIDSAM	0.17*	0.71	0.09	0.22	0.02*	0.07	0.22	0.38	0.13	0.21	0.02*	0.06
SIDMIN	<b>0.12</b>	<b>0.48</b>	<b>0.07</b>	<b>0.12</b>	<b>0.01</b>	<b>0.04</b>	0.29	0.53	0.12	0.16	0.02	0.05
SAMMIN	0.17*	0.64	0.14	0.15	0.02	0.03	0.36	0.78	0.16	0.15	0.03	0.04
SCM	0.21	0.91	0.11	0.27	0.02	0.08	0.20	0.85	0.15	0.37	0.02*	0.06

### 3.2 Accuracy and Precision Values after the Addition of Environmental Noise

Before introducing simulated error from the other sources the offset representing the  $NEAR(\theta)_E$  was applied to one simulation set ( $\theta_s = 19.1^\circ$ ). The results are shown in Fig. 5.

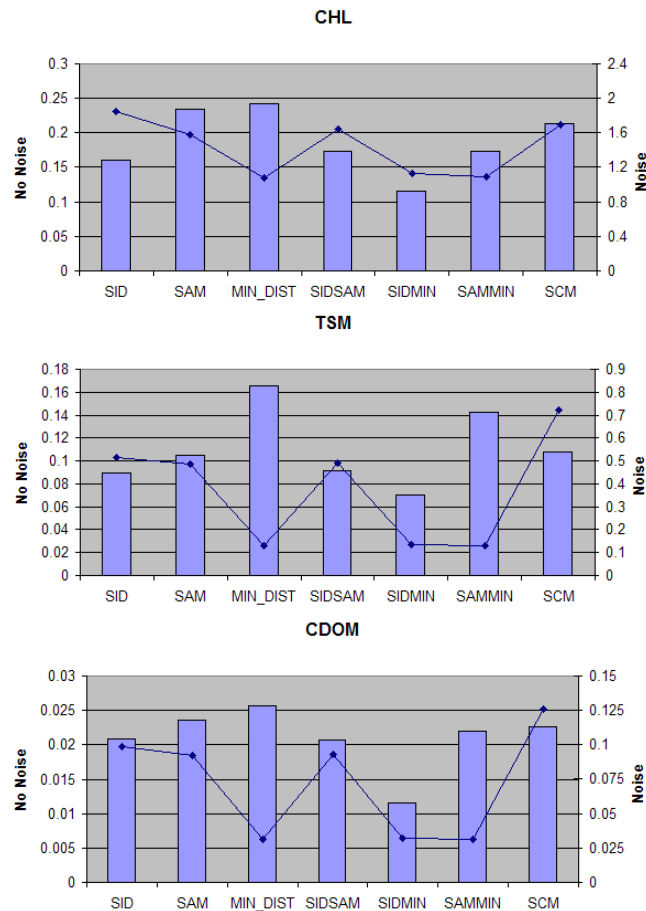


Fig. 5 Mean retrieval accuracy for chlorophyll a, TSM and CDOM with and without added noise. The retrieval was done using the band specific cubic forward model. The bars are the noise free averages and the line is the average after addition of a  $NEAR(\theta)$  of 0.001

Before the addition of the noise it was clear that similarity measures that used SID deliver superior results (Table 3). However, after the addition of the noise the minimum distance measure was the most accurate. The reason for this can be deduced if the effect of the noise on the simulated spectrum is considered. With the SAM and SCM measures the denominator is more sensitive to increases in the large values of the vector than the numerator. The SID, SAM and SCM measures, however, consider the band reflectance value in relation to the other bands within the spectrum. The minimum distance measure will be influenced the most by those bands that have the highest value. The effect of the small change in these large values will be less pronounced so the effect on the retrieval will also be limited.

Sample plots of the atmospheric noise-error relationship are shown in Fig. 6. In general terms the TSM and CDOM retrieval errors behave in the same somewhat exponential manner. In both cases the minimum distance criterion shows the best response in terms of the accuracy and precision, and the SCM measure shows the worst. The apparently less regular relationships between the chlorophyll *a* retrieval errors are deceptive, as almost none of the differences are significant at 95%. Notwithstanding this the precision of chlorophyll *a* retrieval for the minimum distance criterion is on average 2.0, 2.5 and 3.7 times more precise than SCM, SAM and SID respectively.

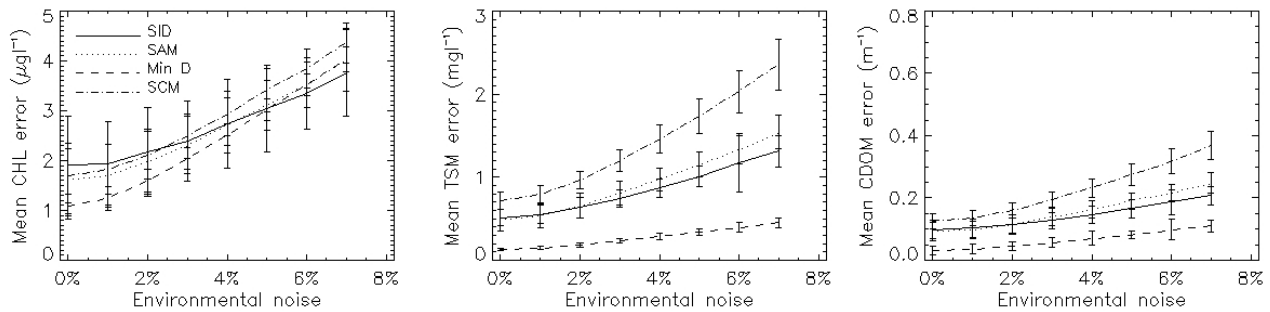


Fig. 6: Average error of hydrosol retrieval, with its 95% confidence intervals, against the environmental noise level for selected weighting schemes.

### 3.3 Accuracy and Precision Values after the Addition of Atmospheric Noise

Sample plots of the atmospheric noise-error relationship are shown in Fig. 7. It is clear that the minimum distance criterion has the greatest sensitivity to the increase in atmospheric noise and the hydrosol error values follow a linear trend with the increase in atmospheric noise whereas the other three criteria appear relatively insensitive to the increase in atmospheric noise. For the SID, SCM and SAM criteria the hydrosol retrieval precision remains constant but the minimum distance criterion has an exponential relationship between the hydrosol retrieval precision and the atmospheric noise.

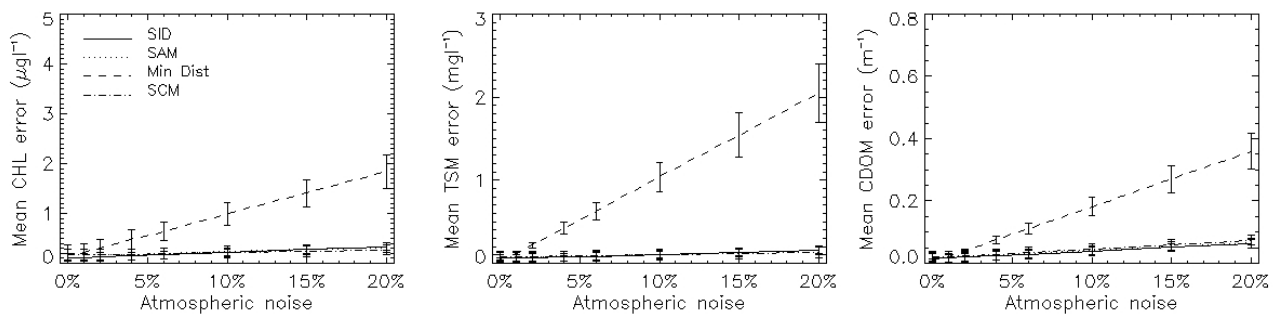


Fig. 7: Average error of hydrosol retrieval, with its 95% confidence intervals, against the atmospheric correction noise level for selected weighting schemes.

### 3.4 Accuracy and Precision Values after the Addition of SIOP Noise

Sample plots of the atmospheric noise-error relationship are shown in Fig. 8. The minimum distance criterion has the greatest sensitivity to the increase in noise, but the difference between it and the other three criteria is greatly reduced. In the case of TSM retrieval there is no discernable difference between the four criteria. The hydrosol retrieval precision varies in proportion to the accuracy.

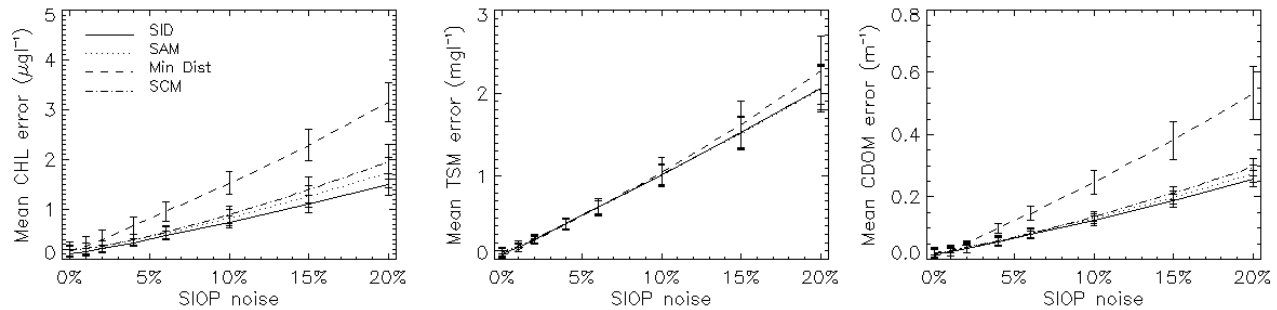


Fig. 8: Average error of hydrosol retrieval, with its 95% confidence intervals, against the SIOIP correction noise level for selected weighting schemes.

## 4 CONCLUSIONS

This paper shows that the use of a band specific value of the anisotropic factor improves the performance of the hydrosol concentration retrieval in terms of accuracy and precision. Furthermore the minimum distance criterion has been shown to be the most resistant to the introduction of environmental noise in general and the  $NEAR(0)_E$  in particular but to perform poorly when noise associated with the atmospheric correction or SIOIP measurement is introduced. Of the other criteria there is no discernable difference between performance of the SID and SAM measures which both have equal or sometimes superior performance to the SCM measure.

## ACKNOWLEDGEMENTS

The authors would like to thank CSIRO for aid in the field work, laboratory work and for assistance with *Hydrolight*® software. In particular we would like to thank Mr Paul Daniel for his assistance in the field operations, Ms Lesley Clementson for the laboratory measurements and Dr Arnold Dekker and Dr Vittorio Brando. We would like to thank the European Space Agency for providing the MERIS FR image under the AO 595 agreement and SEQWater for the provision of historical water quality data.

## REFERENCES

- [1] Ryding, S.-O., Rast, W., and Unesco., [The Control of eutrophication of lakes and reservoirs] Parthenon Pub. Group, Carnforth, Lancs., U.K.(1989).
- [2] Orr, P. T., and Schneider, P. M., [Toxic Cyanobacteria Risk Assessment: Reservoir Vulnerability and Water Use Best Practice] SEQ Water, Brisbane(2006).
- [3] Clementson, L. A., Parslow, J. S., Turnbull, A. R. *et al.*, "Optical properties of waters in the Australasian sector of the Southern Ocean," *J. Geophys. Res.-Oceans*, 106(C12), 31611-31625 (2001).
- [4] WET Labs Inc, [ac-9 Protocol Document (Revision J)] Western Environmental Technology Laboratories (WETLabs), Philomath, OR(2005).
- [5] Maffione, R. A., and Dana, D. R., "Instruments and methods for measuring the backward-scattering coefficient of ocean waters," *Appl. Opt.*, 36(24), 6057-6067 (1997).
- [6] Phinn, S. R., Roelfsema, C., Scarth, P. *et al.*, [An integrated remote sensing approach for adaptive management of complex coastal waters. Final Report - Moreton Bay Remote Sensing Tasks (MR2), CRC for Coastal Zone, Estuary & Waterway Management.] CRC for Coastal Zone, (2005).
- [7] Mobley, C. D., and Sundman, L., [Hydrolight 4.2 Users' Guide.] Sequoia Scientific, Inc., Redmond, WA(2001).
- [8] Pope, R. M., and Fry, E. S., "Absorption spectrum (380 -700 nm) of pure water. II. Integrating cavity measurements," *Appl. Opt.*, 36(33), 8710-8723 (1997).
- [9] Smith, R. C., and Baker, K. S., "Optical properties of the clearest natural waters (200-800 nm)," *Appl. Opt.*, 20(2), 177-184 (1981).

- [10] Gordon, H. R., Brown, O. B., and Jacobs, M. M., "Computed relationships between the inherent and apparent optical properties of a flat homogeneous ocean," *Appl. Opt.*, 14(2), 417-427 (1975).
- [11] Whitlock, C. H., Poole, L. R., Ustry, J. W. *et al.*, "Comparison of reflectance with backscatter and absorption parameters for turbid waters," *Appl. Opt.*, 20(3), 517-522 (1981).
- [12] Morel, A. 1974. "Optical properties of pure water and pure seawater", p. 1-24. *In* N. G. Jerlov and E. Steeman Nielsen [eds.], [Optical aspects of oceanography]. Academic.,(1974).
- [13] Aas, E., "Two-stream irradiance model for deep waters," *Appl. Opt.*, 26(11), 2095-2101 (1987).
- [14] Stavn, R. H., and Weidemann, A. D., "Shape Factors, Two-Flow Models, and the Problem of Irradiance Inversion in Estimating Optical Parameters," *Limnol. Oceanogr.*, 34(8, Hydrologic Optics), 1426-1441 (1989).
- [15] Slade, W. H., Ransom, H. W., Musavi, M. T. *et al.*, "Inversion of ocean color observations using particle swarm optimization," *IEEE T. Geosci. Remote*, 42(9), 1915-1923 (2004).
- [16] Clerc, M., and Kennedy, J., "The particle swarm - explosion, stability, and convergence in a multidimensional complex space," *IEEE T. Evolut. Comput.*, 6(1), 58-73 (2002).
- [17] Du, Y., Chang, C.-I., Ren, H. *et al.*, "New hyperspectral discrimination measure for spectral characterization," *Opt. Eng.*, 43(8), 1777-1786 (2004).
- [18] Carvalho, O. A., and Menezes, P. R., "Spectral Correlation Mapper (SCM): an improvement on the Spectral Angle Mapper," Ninth JPL Airborne Earth Science Workshop, Jet Propulsion Laboratory, Pasadena, California. 65-74 (2000).
- [19] De Haan, J. F., and Kokke, J. M. M., [Remote Sensing Algorithm Development TOOLKIT I: Operationalisation of Tools for Atmospheric Correction of Remote Sensing Data of Coastal and Inland Waters] Beleidscommissie Remote Sensing, (1996).
- [20] Brando, V. E., and Dekker, A. G., "Satellite hyperspectral remote sensing for estimating estuarine and coastal water quality," *IEEE T. Geosci. Remote*, 41(6), 1378-1387 (2003).